

## Numerical and Experimental Study into Forming of the Longitudinal Externally Splined Sleeves by Internally Rotary Ballizing Process

Ayman Ali Abd-Eltwab (0000-0003-0384-771X)<sup>1\*</sup>, Emad A. Fahmy (0009-0007-4065-2344)<sup>2</sup>, Mohamed N. El-Sheikh (0000-0002-9571-7594)<sup>2</sup>, Ahmed M.I. Abu-Oqail (0000-0003-3056-191X)<sup>2</sup>, Hammad T. Elmetwally (0000-0003-0234-6104)<sup>2</sup>, Eman S. M. Abd-Elhalim (0009-0003-8710-8160)<sup>3</sup>

<sup>1</sup>Mechanical Engineering Department, Faculty of Engineering, Beni-Suef University, Beni-Suef 62511, Egypt

<sup>2</sup>Mechanical Department, Faculty of Technology and Education, Beni-Suef University, Beni-Suef 62511, Egypt.

<sup>3</sup>Mechanical Eng. Dep., Faculty of Engineering, Assiut University, Assiut, Egypt

\* Corresponding author Phone: +20-01005728351, E-Mail: [AymanAli@eng.bsu.edu.eg](mailto:AymanAli@eng.bsu.edu.eg)

Longitudinal externally splined parts have garnered increasing attention due to their critical role in power transmission across various industrial applications. This study explores the use of the internally rotating ballizing technique for manufacturing these components. The process was analyzed both experimentally and numerically through a mathematical model. The experimental investigation focused on key process parameters, including die rotational speed (50, 63, 80, 100, 125, 160, 200, 250, and 315 rpm), axial feed rate (0.13, 0.15, 0.18, and 0.21 mm/rev), interference between the balls and the tubular sample (cross in-feed: 2.5, 3.5, 4.5 and 5.5 mm), and initial tube thickness (4, 5, 6 and 7 mm). The study assessed the influence of these variables on the forming load and the quality of the produced longitudinal externally splined sleeves. A numerical model was developed to predict forming loads, and the findings indicated that these parameters significantly affect both (forming load and filling ratio). The optimal values for these variables were identified, and the numerical results showed a strong correlation with experimental findings.

**Keywords:** Externally splined sleeves, Rotary ballizing process, Numerical method, Experimental study, Forming load

### 1 Introduction

Ballizing is a precision machining technique employed to enhance the surface quality and dimensional precision of cylindrical bars or shafts. This process is primarily employed in manufacturing and engineering industries where achieving precise fits and tolerances is crucial for the proper functioning of mechanical components. Ballizing is particularly useful when dealing with parts that require a high degree of roundness, smoothness, and tight clearances, such as bearings, bushings, and hydraulic or pneumatic cylinders.

For an extended period, the conventional spinning technique has been employed to manufacture axis-symmetric shapes and short tubular items with limited length-to-diameter ratios. To overcome this challenge, significant advancements have been made in tube manufacturing technology. The spinning process has been modified to produce long, small-diameter tubes from difficult-to-form materials such as CP titanium, Incoloy 825, Inconel 600, and Stainless Steel AISI-304. Notably, ball spinning, a specialized process for producing thin-walled, small-diameter tubes, has become widely used in recent years, despite being

invented several decades ago [1].

Many researchers are working on developing various types of equipment to meet the evolving demands. Research on innovative process configurations in spinning has revealed significant potential for advancements. This process can offer greater flexibility, enable the production of a wider variety of shapes, and accommodate more challenging materials [2].

The significant influence of two main parameters, the workpiece diameter ratio ( $D_1/D_2$ ) and feed rate ( $v$ ) must be considered when evaluating the damage behavior observed during ball rotation operations [3]. It was established that smaller ball diameters result in higher levels of stress and strain, along with increased strain rates. Numerical analysis further reveals that the reduction ratio plays a significant role in shaping the strain state within the inner tube holes after the ballizing process [4,5].

There exists a critical interference value that maximizes the improvement in microhardness, roundness, and surface finish during the ballizing process [6]. Generally, increasing the interference (the gap between the ball tool and the bore) improved surface quality up to an optimal point [7,8]. Other factors such as the attack angle and pivotal feed were

observed to reduce axial force and raw material accumulation [9–11].

Key variables such as tool rotational speed, pivotal feed, and cross in-feed were found that have a significant influence in both the forming force and goodness of the formed sleeves, surfaces roughness of sleeves decrease with interference raise [12–18]. While it raises with increasing pivotal feed. The filling rate increases by rising both interference and pivotal feed [19]. It was discovered that speed and feed are the most critical variables impacting power usage. The resulting force on cylinder is governed by the cylinder offensive angle, cylinder snout radius, and reduction % [20].

The modern progress in tubular parts spinning spinning for both large and small inner grooved tubes, as well as internal toothed tubes, face multiple challenges. Most significant of these comprise material accumulated in front of the deformation balls, raw material folding at the internal surface of the tube and forming tool breakdown due to load variations at the forming teeth root. While these problems have been treated individually in the literature, there has yet to be a comprehensive method to tackle all of them simultaneously [21–23].

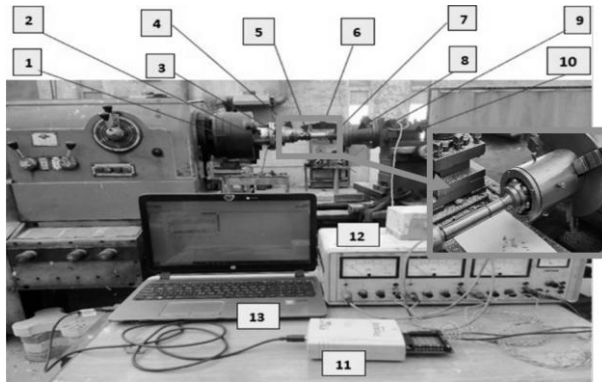
In this research suggests a novel design that promises to address all these problems simultaneously using simple tools to produce external gears or any other externally toothed parts. In addition to the formation of tubular sections with relatively large thicknesses compared to previous studies in the spinning of internally splined or non-splined tubes. Also, analytical, and practical work is done to examine the formation of externally toothed components utilizing a new rotating ballizing approach.

## 2 Experimental work

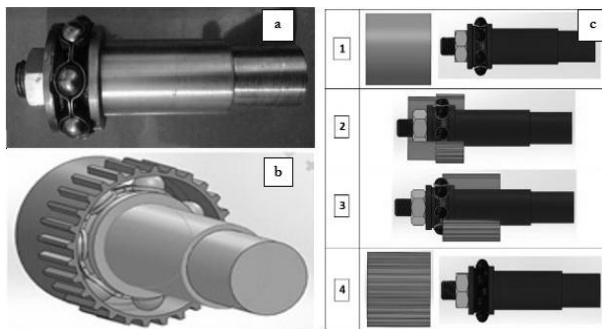
The experimental test rig was designed and coupled with a data acquisition system for a continuous measuring and monitoring the investigated load of forming process. An experimental work for produce the longitudinal Externally-Splined Sleeves using conventional universal lathe machine with new technique and new tool is carried out was supported on tool holder which fixed on dynamometer device which fixed on special holder which fixed on Tool post for this universal lathe machine, this dynamometer connected with data logger device which connected the computer for measuring the forming loads. This section presents description for the experimental setup. That included forming tool description, instruments used in forming process such as center lathe machine, force measurement devices and its calibration, specimen preparation and blank material, preparation of forming process and data reduction, and setting up and description of the process. Also, all technical specifications of tool, instruments, and the used measuring devices.

## 3 Forming tools

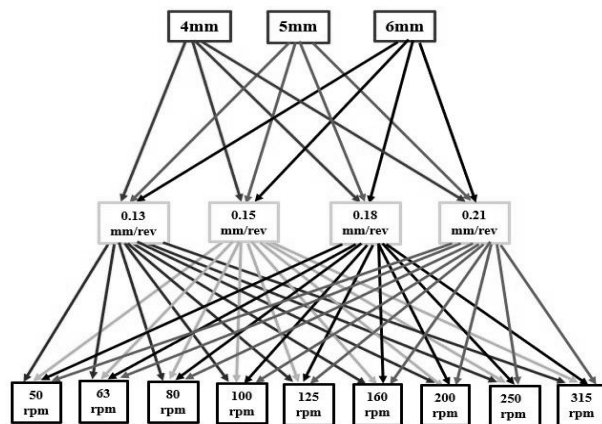
At the beginning the experiments in this study were conducted using two types of forming tools. The first type includes a group of mandrills with ball bearings with different outer diameters and various balls diameters, the other type has a different design, each ball bearing is mounted on a separate mandrel. Fig.1 photo showing the general arrangement of experimental equipment used to form longitudinal externally splined sleeves, which consists of lathe chuck numbered in (1), (2) product ejection mechanism, (3) toothed die, (4) specimen, (5) forming balls, (6) novel ballizing tool, (7) tool holder, (8) dynamometer, (9) holding jig, (10) tool post, (11) data logger device (12) transducer device and (13) laptop. Fig. 2 a, b, c depicts the first forming tool used in form externally toothed parts and the sequence of the process. Numerous experiments have been conducted using all types of ball bearings with different outer diameters, to check the best ball bearing with outer diameter that provides suitable interference with the different thicknesses proposed for the specimens, as well as the appropriate ball diameter. which gives the best result in forming the product as preliminary experiments. The first tool is a single ball bearing with a suitable outer diameter, which was chosen based on the preliminary experiments that were carried out with different diameters as we mentioned previously. the outer cage of these bearings used in the initial experiments was removed and prepared in a specific way, and it will be shown in Fig. 2 a, b while Fig. 2 c schematic drawing of ballizing process sequence, Fig. 3 Schematic drawing of parameters study in forming ballizing process, Fig. 4 shows modern single-stage mandrel and Fig. 5 Schematic drawing for load components of novel rotary ballizing technique used to form longitudinal externally splined sleeves, while when used with larger thicknesses (greater interference between the balls and the sample). It had a collapse such as warp or a fracture of the inner net containing the balls, and the balls fell during the forming process. This led to replacement first ball bearing type with the new second type, which has one stage of the ball bearing as well, but with high design specifications and durability, in order to perform the tasks required of it to the fullest even with larger thicknesses, it gave very excellent experimental results. where the tubular stock will be a rotational floating block, which will force the metal tube to penetrate into the die cavity. the forming tool was supported on tool holder which fixed on dynamometer device which fixed on special holder which fixed on tool post. a simple center lathe carriage, concentric with its centerline. The die takes its variable speed from the center lathe chuck. Meanwhile, the mandrel with rotating balls moves in a linear motion to give the automatic axial feeding by the lathe carriage as shown in Fig. 1.



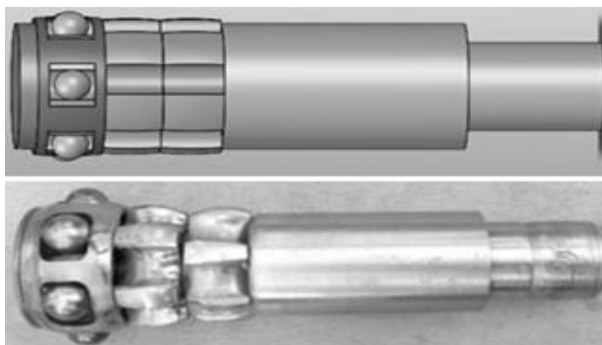
**Fig. 1** A photo showing the general arrangement of experimental equipment used to form longitudinal externally splined sleeves



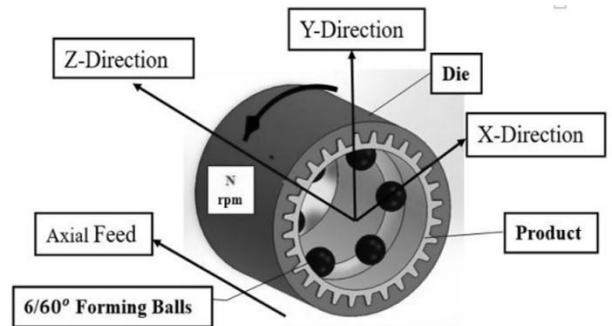
**Fig. 2** Depicts the first forming tool used in form externally toothed parts and the sequence of the process



**Fig. 3** Schematic drawing of parameters study in forming ballizing process



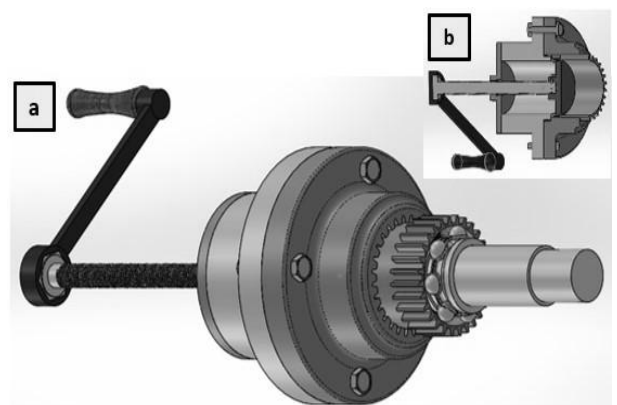
**Fig. 4** A picture showing modern single-stage mandrel



**Fig. 5** Drawing for load components of novel rotary ballizing technique used to form longitudinal externally splined sleeves

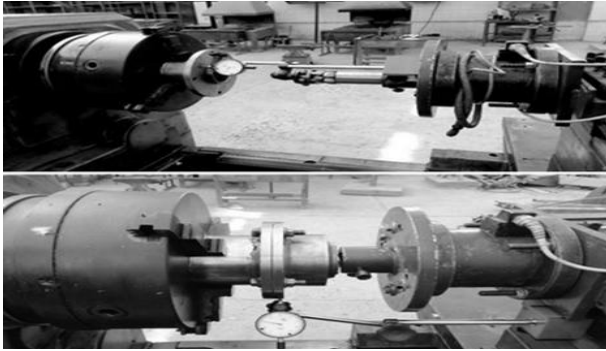
#### 4 Ball forming adjusting mechanism

The ball bearing assembly was mounted on the mandrel and consisted of six balls, each with a diameter of 16 (mm) arranged in a single level, the angle between each ball and the other is 60 degrees. During the forming process, the balls are free to rotate in any direction due to frictional contact with the specimen surface. This rotational freedom facilitates smooth metal flow, reduces forming loads, minimizes material accumulation, and prevents surface peeling. The flexibility of the rotating balls allows for uniform metal distribution and enhanced penetration of the material into the die's complex tooth cavities, thereby improving the filling ratio and ensuring high-quality surface integrity of the formed product as shown in Fig. 6 a, b.



**Fig. 6** Isometric view of the forming tool, illustrating the process description and the mechanism of product ejection

To guarantee precise alignment, the mandrel's centrality was adjusted relative to the lathe chuck using a dial gauge indicator with an accuracy of 0.01 mm, as shown in Fig. 7. This alignment ensured that the mandrel, die, and specimen shared the same rotational axis (lathe axis), maintaining uniform wall thickness and preventing any lateral displacement of the mandrel. Misalignment could otherwise cause internal distortion of the tubular specimen and potential erosion of the die tooth stems if the deviation exceeded the permissible limit.



**Fig. 7** Calibration the centrality of the die and tools with the centrality of the lathe using dial gauge indicator

## 5 Numerical analysis of the single stage ballizing technique

Consider the matter of estimating a function's values at unlisted points, based on the experimental data

$$P_n(x) = y = a_n x^n + a_{n-1} x^{n-1} + \dots + a_1 x + a_0 \quad (1)$$

The polynomial of degree  $n < m - 1$ , using least squares procedure is handled similarly. We choose the

$$E = \sum_{i=1}^m (y_i - P_n(x_i))^2 \quad (2)$$

$$= \sum_{i=1}^m (y_i)^2 - 2 \sum_{i=1}^m P_n(x_i) y_i + \sum_{i=1}^m (P_n(x_i))^2 \quad (3)$$

$$= \sum_{i=1}^m (y_i)^2 - 2 \sum_{i=1}^m \left( \sum_{j=0}^n a_j (x_i)^j \right) y_i + \sum_{i=1}^m \left( \sum_{j=0}^n a_j (x_i)^j \right)^2 \quad (4)$$

As in the linear case, for  $E$  to be minimized it is the necessary that  $\partial E / \partial a_j = 0$ , for each  $j = 0, 1, \dots, n$ . Thus, for each  $j$ , we must have:

$$0 = \frac{\partial E}{\partial a_j} = -2 \sum_{i=1}^m \left( \sum_{j=0}^n y_i (x_i)^j \right) + 2 \sum_{i=1}^m a_k \sum_{j=0}^n (x_i)^{j+k} \quad (5)$$

This gives  $n + 1$  normal equations in  $n + 1$  unknowns  $a_j$ . These are:

$$\sum_{k=0}^n a_k \sum_{i=1}^m (x_i)^{j+k} = \left( \sum_{i=1}^m y_i (x_i)^j \right) \quad (6)$$

For each  $j = 0, 1, \dots, n$  and for it is helpful to write the equations as follows:

$$a_0 \sum_{i=1}^m x_i^0 + a_1 \sum_{i=1}^m x_i^1 + a_2 \sum_{i=1}^m x_i^2 + \dots + a_n \sum_{i=1}^m x_i^n = \sum_{i=1}^m y_i x_i^0 \quad (7)$$

$$a_0 \sum_{i=1}^m x_i^1 + a_1 \sum_{i=1}^m x_i^2 + a_2 \sum_{i=1}^m x_i^3 + \dots + a_n \sum_{i=1}^m x_i^{n+1} = \sum_{i=1}^m y_i x_i^1 \quad (8)$$

$$a_0 \sum_{i=1}^m x_i^n + a_1 \sum_{i=1}^m x_i^{n+1} + a_2 \sum_{i=1}^m x_i^{n+2} + \dots + a_n \sum_{i=1}^m x_i^{2n} = \sum_{i=1}^m y_i x_i^n \quad (9)$$

Least squares polynomial:

$$f(x) = y = a_0 + a_1 x + a_2 x^2 \quad (10)$$

Fit the data in following Table 1 with discrete Least Square Polynomial of degree at most 2. Where:  $n = 2, m = 3$  and  $y = f(x) = a_0 + a_1 x + a_2 x^2$ .

in Tab. 1. Fig. 7 presents a graph of the values in Tab. 1 and Tab. 2. from this graph, it seems the actual relation between  $x$  and  $y$  is linear. The likely reason that no line precisely matches the data is because of inaccuracies within the data. Thus, it's imprudent to require the approximating function to perfectly align with the data. In fact, such a function would generate oscillations that weren't initially there. As an illustration, the graph of the ninth degree interpolating polynomial shown in undone strained mode for the data in Tab. 3 is obtained in maple with the command.

## 6 Polynomial least squares for numerical forming load

The overall difficulty of approximating a dataset,  $\{(x_i, y_i), i = 1, 2, \dots, m\}$ , with an algebraic polynomial in general form like the following as reference [24].

constants  $a_0, a_1, \dots$  and  $a_n$  to minimize least squares error  $E = E_2(a_0, a_1, \dots$  and  $a_n)$ , where:

$$ma_0 + a_1 \sum_{i=1}^m (x_i) + a_2 \sum_{i=1}^m (x_i^2) = \sum_{i=1}^m (y_i) \quad (11)$$

$$a_0 \sum_{i=1}^m (x_i) + a_1 \sum_{i=1}^m (x_i^2) + a_2 \sum_{i=1}^m (x_i^3) = \sum_{i=1}^m (x_i y_i) \quad (12)$$

$$a_0 \sum_{i=1}^m (x_i^2) + a_1 \sum_{i=1}^m (x_i^3) + a_2 \sum_{i=1}^m (x_i^4) = \sum_{i=1}^m (x_i^2 y_i) \quad (13)$$

**Tab. 1** The forming load values against die rotating speed

i	1	2	3
N(rpm)	50	63	80
F <sub>t</sub> (kN)	3.59922	6.962552	5.081034

**Tab. 2** The data to fitting curve for forming load

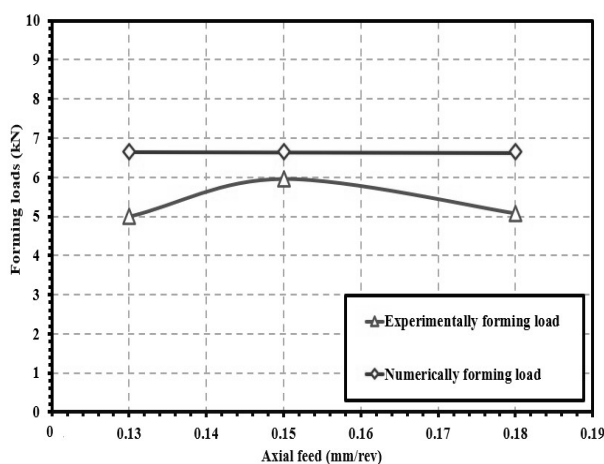
m	$x_i$	$y_i$	$x_i^2$	$x_i^3$	$x_i^4$	$x_i y_i$	$x_i^2 y_i$
	f(mm/rev)	F <sub>t</sub>					
1	0.13	6.726326	0.0169	0.002197	0.00028561	0.87442238	0.113674909
2	0.15	6.964957	0.0225	0.003375	0.00050625	1.04474355	0.156711533
3	0.18	7.391146	0.0324	0.005832	0.00104976	1.33040628	0.23947313
Σ	0.46	21.082429	0.0718	0.011404	0.00184162	3.24957221	0.509859572

Form the data was tabulate in Tab. 2 can be calculate and solve of the equations to presented in Graph 1. Thus, the forming load or least squares polynomial

of degree 2 fitting the data in Tab. 3 is whose graph is shown in Graph 1 at the given values of  $x_i$  we have the approximations shown in Tab. 3 and Tab. 4.

**Tab. 3** The data to fitting curve for numerically and experimentally forming load with the errors at all points

i	1	2	3
$x_i$ (f(mm/rev))	0.13	0.15	0.18
$y_i$ (F <sub>t</sub> )	4.9922	5.962552	5.081034
$P(x_i)$	6.647098	6.64659946	6.6458524
$y_i - P(x_i)$	-1.6549	-0.68404746	-1.5648184
E%	-3.1497	-11.4723941	-3.797242

**Graph 1** Comparison between computed numerically and experimentally forming load results data for axial feed

## 7 Result and discussion

The experimental work executed through the present study resulted in measurable variables. Derived quantities were calculated based on these measured variables. In this chapter, a comprehensive discussion of the experimental results is presented. A series of experiments was conducted to examine the effects of process parameters ( $t$ ,  $\Delta t$ ) and machine parameters ( $f$ ,  $N$ ) on deformation loads. These effects were analyzed as a function of interference, pivot feed, and tube thickness. Additionally, another set of experiments was performed to investigate the influence of process and machine parameters on the quality of the toothed tubular product. The product quality was evaluated based on the filling ratio of the external teeth and the hardness of the teeth.

While Tab. 4 Clarify the experiments executed and operating parameters for single-stage ballizing technique. The forming load required to deformation of tubular parts with external teeth depends on many variables of the process and machine parameters such as die speed, axial feed, ball diameter, thickness of tube, and interference among outer diameter of ball bearing and inner diameter of the tubular sample. The effect of these parameters on forming loads, quality of product, filling ratio and hardness of teeth. A tensile and compressive test was conducted for







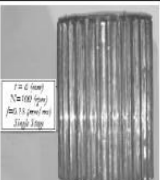

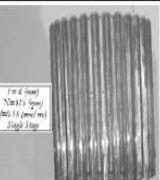
standard lead samples to determine the mechanical properties of the metal before forming, such as the maximum tensile and compressive stress of the metal, the strain hardening coefficient, the toughness coefficient, etc. In addition to conducting a hardness test for the metal before forming and comparing it to the hardness of the samples after forming under different working conditions of the process. in addition, comparison between the computed and the experimental results and discussed.

**Tab. 4** Clarify the experiments executed and operating parameters for single-stage ballizing technique

Investigation parameters	Values
Die rotational speed (N)	(50, 63, 80, 100, 125, 160, 200, 250, and 315 rpm)
Axial feed (f)	(0.13, 0.15, 0.18 and 0.21 mm/rev)
Cross in feed (interference) ( $\Delta t$ )	(2.5, 3.5, 4.5 and 5.5 mm)
Initial tube thickness (t)	(4, 5, 6 and 7mm)

## 8 Externally toothed tubular product




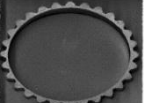


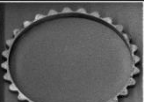
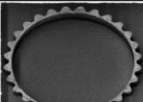
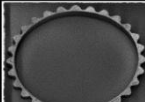
**Tab. 5** Illustrates some externally toothed tubes formed at various speeds, feeds, and filling ratios

Speed Feed	N=100 (rpm)	N=200 (rpm)	N=315 (rpm)
f=0.13 (mm/rev)			
f=0.15 (mm/rev)			
f=0.18 (mm/rev)			

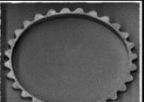
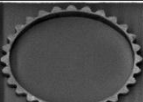
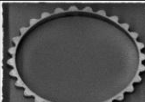
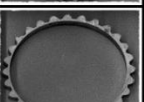
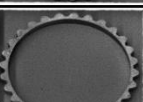
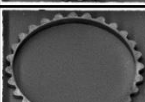
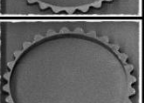
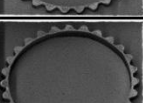
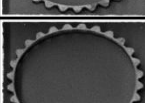
Tab. 5 illustrates some externally toothed tubes formed at various speeds, feeds, and filling ratios. Correspondingly, Tab. 6, 7, and 8 illustrate the scanned cross-sectional profiles of the samples produced under varying cross-infeed depths, axial feed rates, and die rotational speeds. The obtained results clearly indicate that the proposed rotary ballizing process enables the precise and uniform formation of externally toothed tubular geometries. this newly developed method represents an innovative and cost-efficient forming approach, characterized by its simplicity, minimal tooling requirements, and superior utilization of time, energy, and material resources when compared

with conventional manufacturing techniques. Representative samples of the externally toothed tubular products fabricated using the rotary ballizing tool are shown in Figs. 8 a, b.


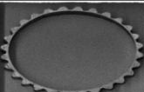
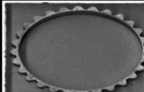
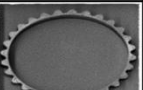
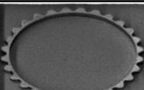
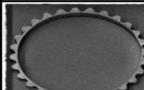
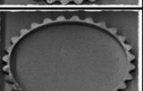
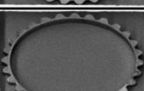
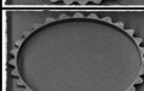
**Tab. 6** A photo scan for toothed tube products at N=63 (rpm), pivot feed, and cross in feed

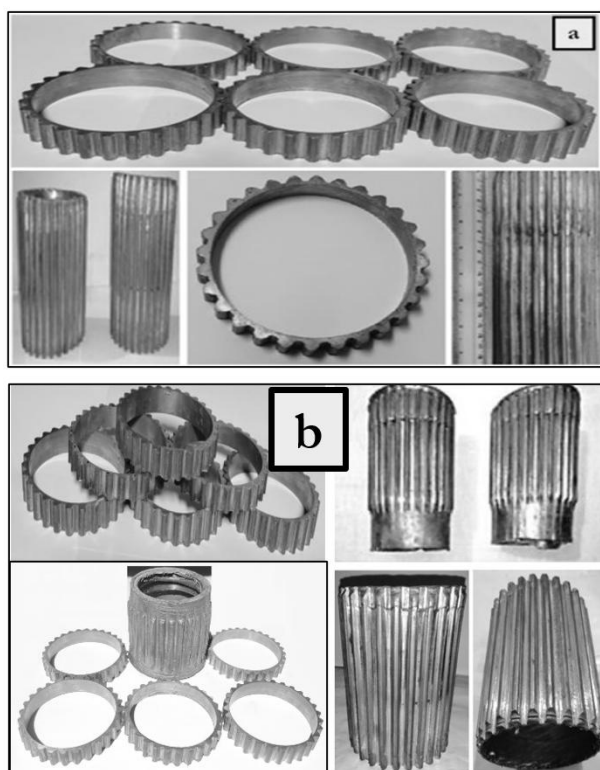
		$\Delta t=2.5\text{mm}$	$\Delta t=3.5\text{mm}$	$\Delta t=4.5\text{mm}$
N = 63 rpm	f = 0.13 mm/rev			
	f = 0.15 mm/rev			
	f = 0.18 mm/rev			

**Tab. 7** A photo scan for toothed tube products at N=80 (rpm), pivot feed, and cross in feed

		$\Delta t=2.5\text{mm}$	$\Delta t=3.5\text{mm}$	$\Delta t=4.5\text{mm}$
N = 80 rpm	f = 0.13 mm/rev			
	f = 0.15 mm/rev			
	f = 0.18 mm/rev			

**Tab. 8** A photo scan for toothed tube products at  $N=100$  (rpm), pivot feed, and cross in feed

		$\Delta t=2.5\text{mm}$	$\Delta t=3.5\text{mm}$	$\Delta t=4.5\text{mm}$
$N=100\text{ rpm}$	$f=0.13\text{ mm/rev}$			
	$f=0.15\text{ mm/rev}$			
	$f=0.18\text{ mm/rev}$			



**Fig. 8** Some of the externally toothed tubular products produced with the new rotary ballizing tool

## 9 Relationship among load and ball displacement

Graphs 2, 3, and 4 illustrate the punch load-displacement relationship, where the curve appears somewhat irregular. To better understand this behavior, the mandrel stroke can be divided into three distinct stages:

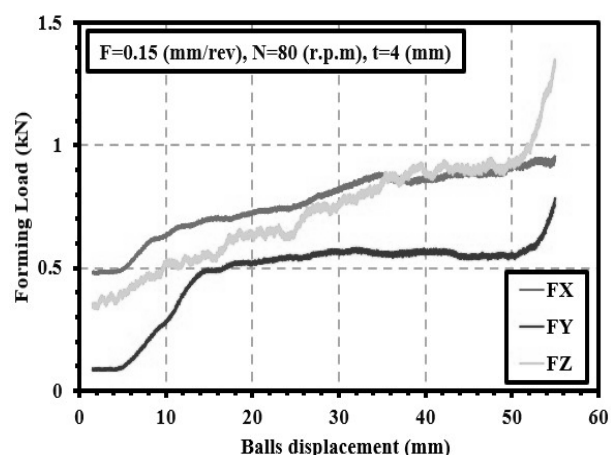
1. Initial Stage (Linear Phase): This stage begins at the onset of the process and continues until the tube sample is fully pressed into the die cavity. During this phase, the forming balls of the mandrel push the sample into the cavity. The deformation loads ( $F_T$ ) can be analyzed into three components: ( $F_x$ ,  $F_y$ , and  $F_z$ ). These forces facilitate metal flow

into the die ribs while simultaneously stretching the specimen in the z-direction. The total load is divided into two main parts:

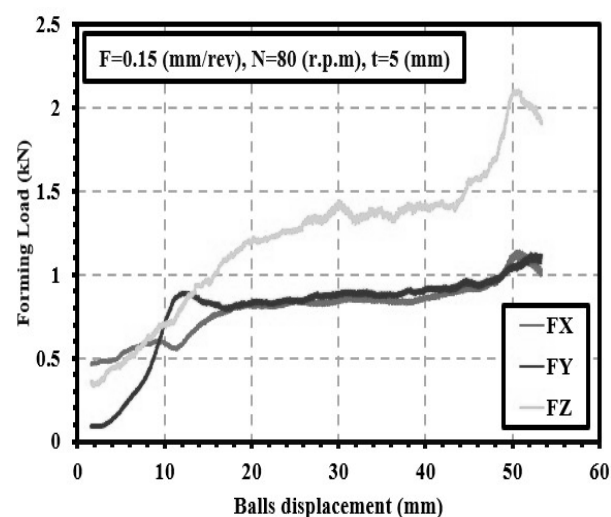
- Coining Load: Required to force the material into the die grooves.
- Spinning Load: Required to induce shear flow within the internal layers of the metal tube, where the tooth shape begins to form.

2. Spinning Stage: This phase represents the actual formation of the toothed tube. Here, the load increases gradually as the toothed profile develops. The increase in load is attributed to both material deformation and friction between the forming balls, the sample, and the die.

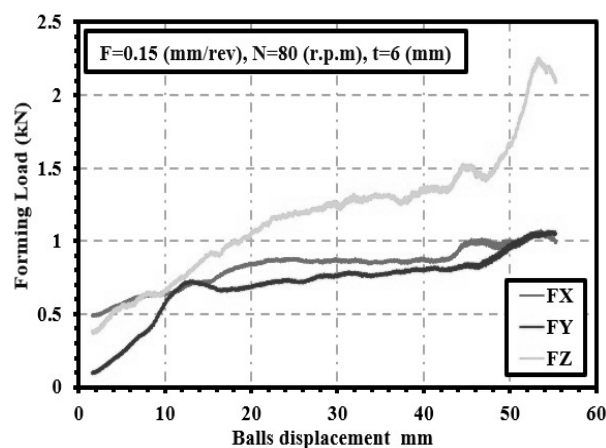
3. Final Stage (Intensive Load Increase): At this point, a significant rise in load occurs due to the accumulation of excess material at the inner end of the die. Spinning this excess material requires a high force, causing the load to continue increasing until the complete formation of the toothed part is achieved.



**Graph 2** Forming load, vs balls displacement at thickness 4(mm)

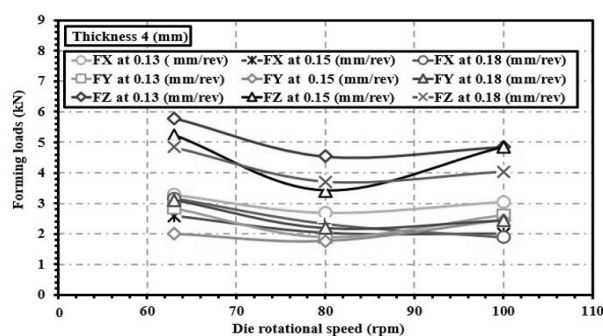


**Graph 3** Forming load, vs Balls displacement at thickness 5(mm)

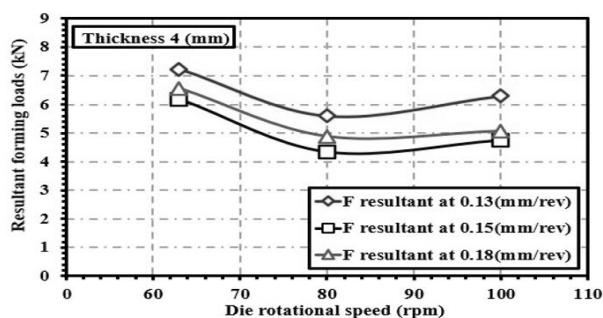


**Graph 4** Forming load, vs balls displacement at thickness 6(mm)

### 10 Influence of the die rotational speed on forming loads



(a)

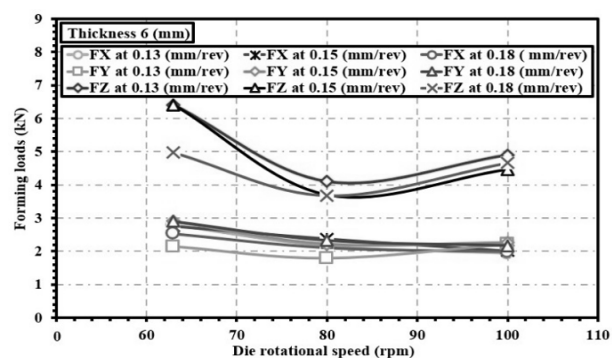


(b)

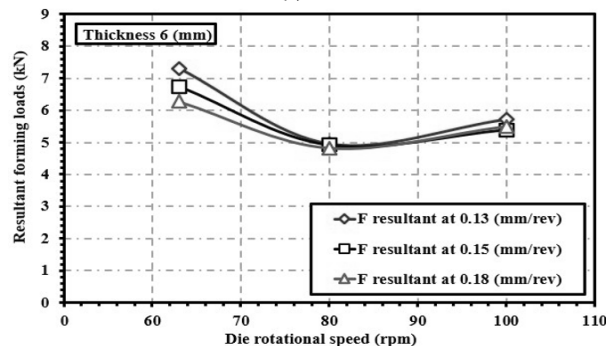
**Graph 5** Relationship between the rotational die speed and forming loads at cross in-feed 2.5(mm)

Graphs 5 a, b, 6 a, b and 7 illustrate the relationship among the die rotational speed and the forming loads with different cross in-feed 2.5, 3.5, 4.5 and 5.5 mm and feeds 0.13, 0.15, 0.18, and 0.21 mm/rev at thickness 4, 5 and 6 mm. It is shown from the curves that, the rotational speed increased, the forming loads decreased in three directions. this is believed to be due to the heat plasticization of the metal resulting from the rapid friction between the forming balls and the sample. which promotes flow, as well as the quick decrease of buildup metal, which lead to lower resistance to deformation. The shorter contact time

between the tool and the workpiece also contributes to minimizing both axial and tangential load components. The optimum speed was found at 200 to 315 rpm during which the load remained constant throughout this range, and therefore this range of speeds gives the manufacturer freedom to choose the optimal speed appropriate for him according to the capabilities of the machine available to it. therefore, the production time decreases as the chosen speed increases, and the cost also decreases. The maximum load found that at 63 rpm. It believed that, at lower rotational die speed the straining of wall thickness will be occurred. These findings agree with previous studies reporting that higher rotational speed improves metal flow and increases cavity filling due to enhanced local pressure and reduced pile-up [11].

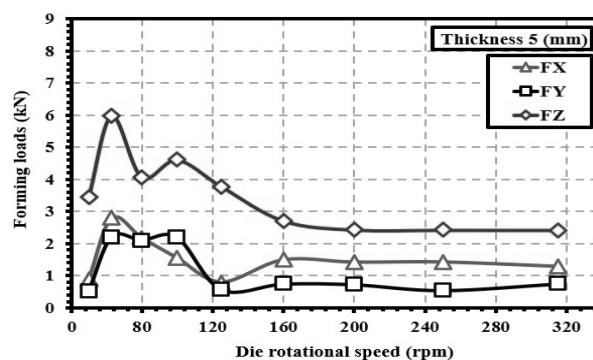


(a)



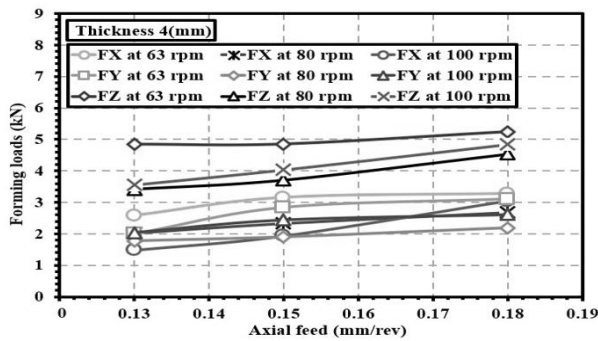
(b)

**Graph 6** Relationship between the rotational die speed and the forming loads at cross in-feed 4.5(mm)

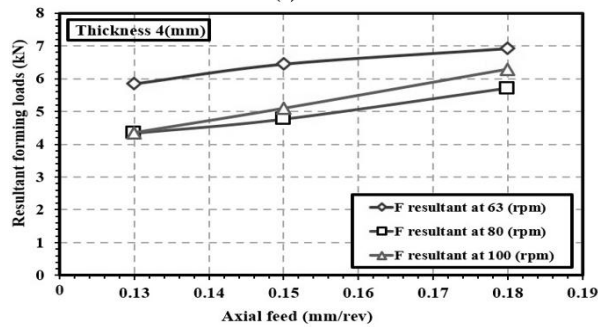


**Graph 7** Relationship between the forming loads versus all speeds

## 11 Effect of mandrel axial feed on forming loads

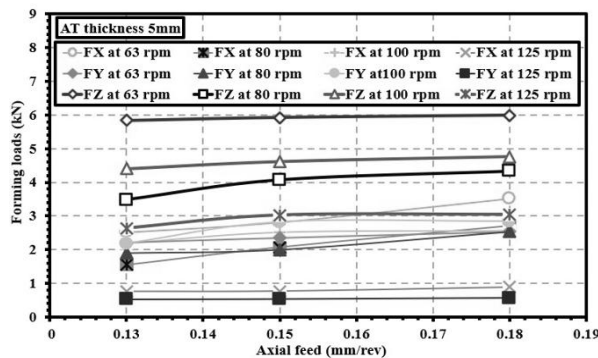


(a)

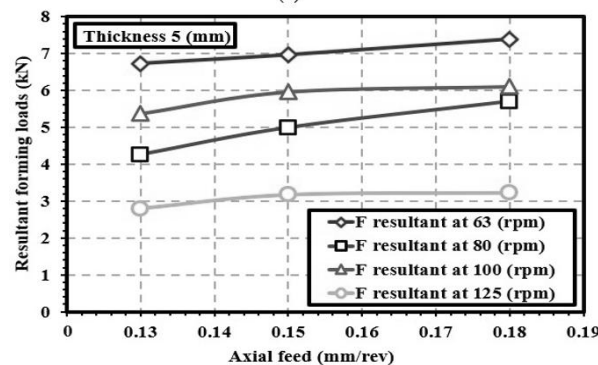


(b)

**Graph 8** Three components of forming load and resultant load versus axial feed at 2.5 (mm) cross in-feed



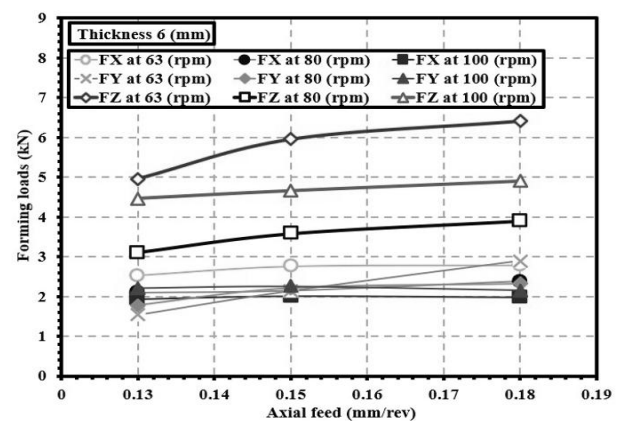
(a)



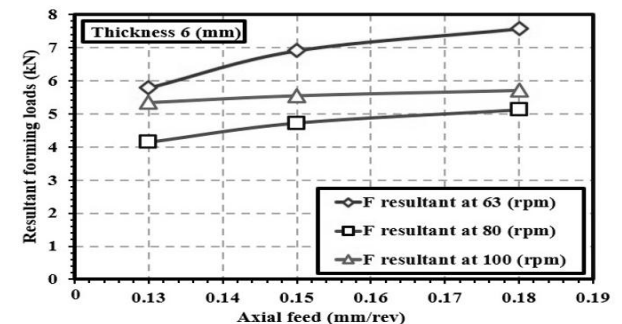
(b)

**Graph 9** Three components of forming load and resultant load versus axial feed at cross in-feed 3.5(mm)

The forming load increased as the axial feed increased at different cross in-feed values (2.5, 3.5, and 4.5 mm). This is likely due to the expansion of the contact area with the rise in axial feed, leading to greater material accumulation (piling up). Consequently, this accumulation contributes to an increase in the forming load components. higher strain rate and reduced thermal softening of the material. Increased friction and metal pile-up in front of the forming balls also contribute to higher axial and tangential loads. Additionally, excessive axial feed can cause unstable metal flow, leading to irregular deformation and greater overall forming forces as shown as in Graphs (8 a, b, 9 a, b and 10 a, b). The obtained results and the trend of the curves concerning the effect of axial feed on the forming loads are in good agreement with the experimental findings reported by [11, 25, 26].



(a)



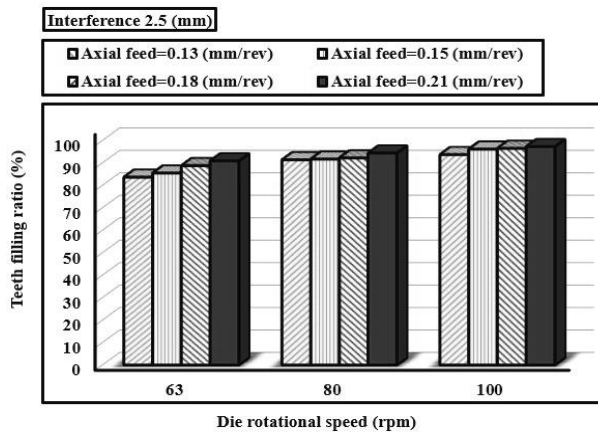
(b)

**Graph 10** Three components of forming load and resultant load versus axial feed at 4.5 (mm) cross in-feed

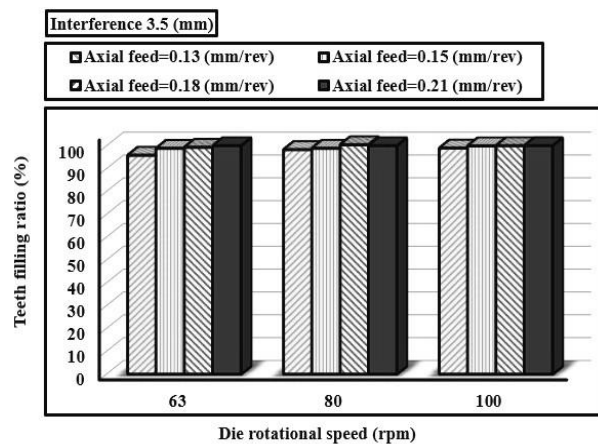
## 12 Influence the die rotational speed on filling ratio of die tooth cavities

The teeth filling ratio against die rotational speed is shown in Graphs 11, 12 and 13 at different cross in-feed (interference) and different axial feed. The filling ratio was increased with increasing the die speed as shown. This is due to the increasing metal flow with high die rotational speed, because of the increase in the temperature of the metal and its plasticity as outcome rapid friction. The higher shear rate enhances

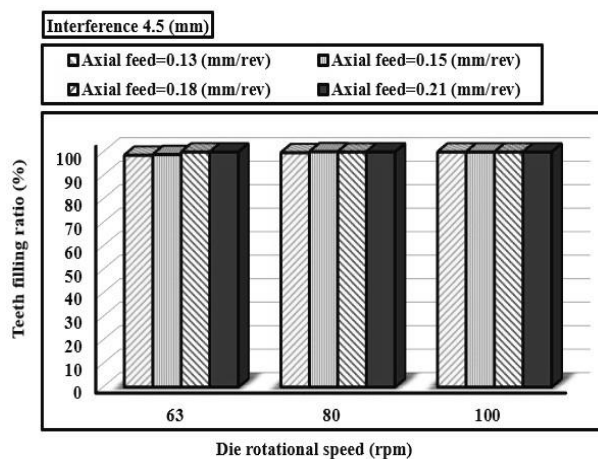
metal flow and reduces pile-up ahead of the balls, ensuring more uniform filling. Moreover, with increasing the die rotational speed the forming balls are forcing more metal at the front and to the inner perimeter of the die it, this gives results more filling for the die teeth cavities. These findings are consistent with the observations reported by [11, 26].



**Graph 11** Die rotational speed vs filling ratio at thickness 4 (mm)

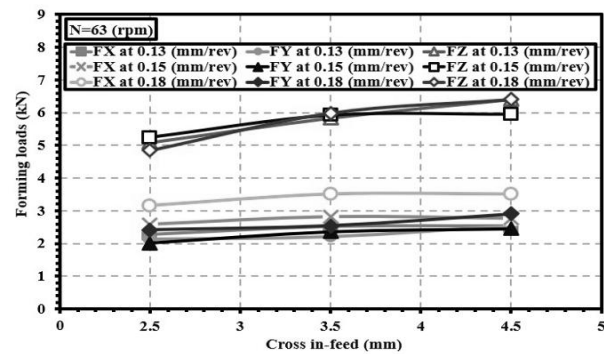


**Graph 12** Die rotational speed vs filling ratio at thickness 5 (mm)

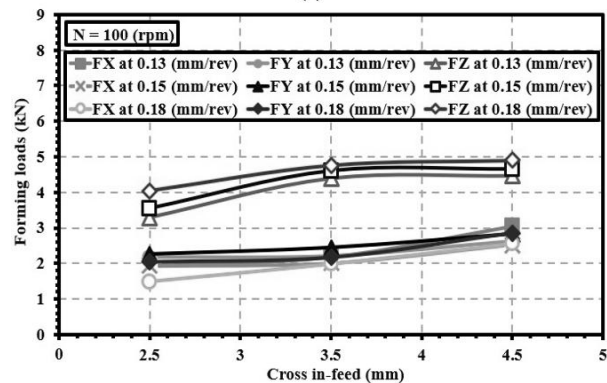


**Graph 13** Die rotational speed vs filling ratio at thickness 6 (mm)

### 13 Influences of diagonal interference on forming load and the filling ratio

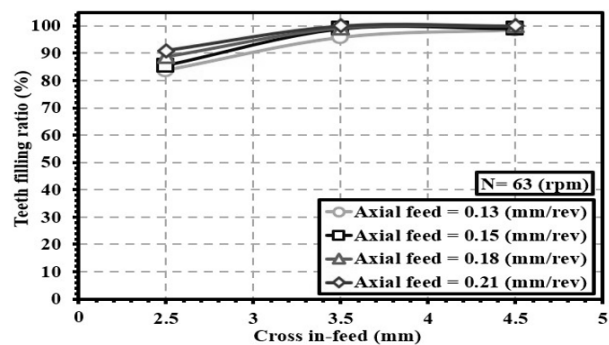


(a)

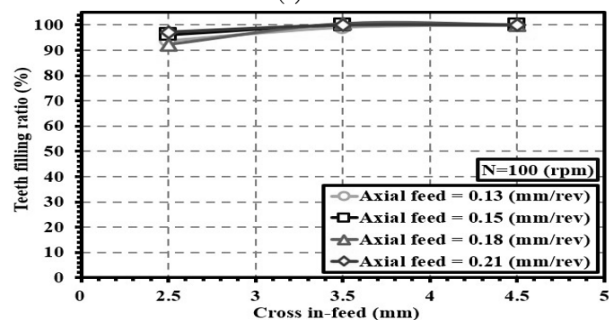


(b)

**Graph 14** Relationship between diagonal interference vs forming load



(a)



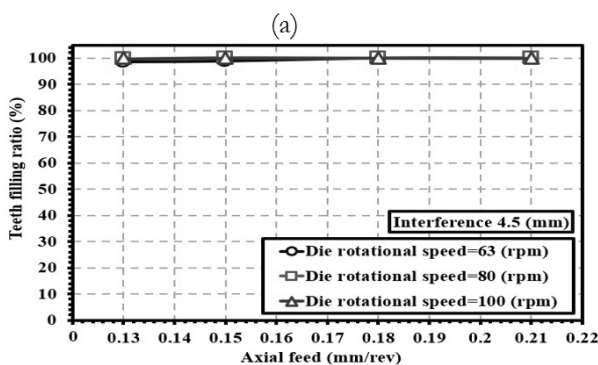
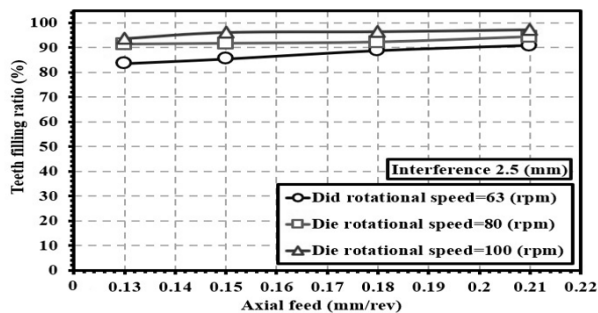
(b)

**Graph 15** Relationship between diagonal interference vs the filling ratio

Graphs 14 a, b and 15 a, b illustrate that as the cross in-feed increases, the forming load also rises due to the expanded contact area and accumulated metal, greater plastic deformation resistance and increased contact pressure. However, excessive interference may cause surface defects and tool wear. An optimal interference value ensures sufficient material flow, accurate tooth filling, and stable forming conditions. Additionally, a higher interference (cross in-feed) enhances the filling ratio of the die tooth cavities due to a greater amount of displaced metal filling the die cavities. The maximum filling ratio of 100% was achieved at cross-feed values of 3.5, 4.5, and 5.5 mm across most speeds and feed rates. These results are in good agreement with the findings of [11, 26].

#### 14 Influence the axial feed on filling ratio of die tooth cavities

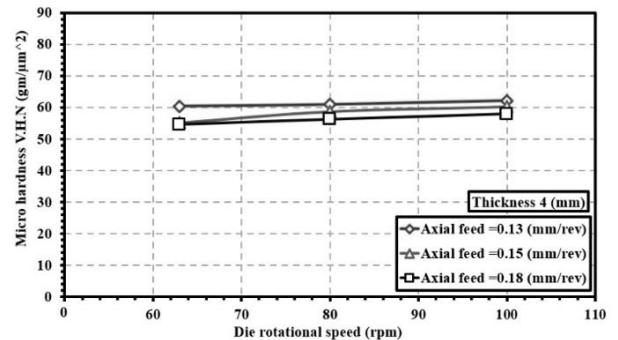
Graphs 16 a, b illustrates that the filling ratio was enhanced by raising the axial feed, as illustrated. where it is with increasing the axial feed results in an increased filling ratio, which is believed to as the axial feed increases, a greater amount of material is pushed toward the forming zone, forcing the metal more effectively into the die cavities. This enhances plastic deformation and improves the filling efficiency. Additionally, higher axial feed reduces excessive metal pile-up in front of the forming balls and promotes smoother material flow, resulting in a higher filling ratio of the splined die cavities. This finding agrees with the observations of El-Sheikh, M. N., et al [11].



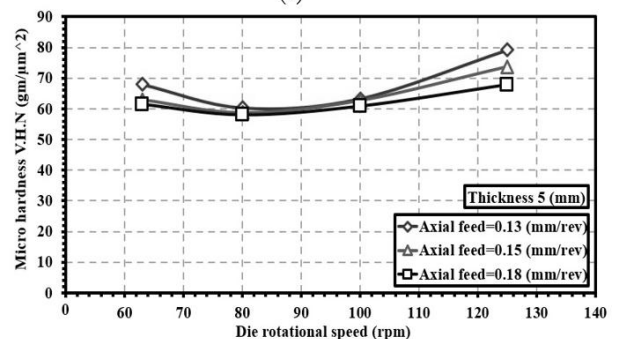
**Graph 16** Effect of axial feed on tooth filling ratio at interference 2.5, 3.5 (mm)

#### 15 Impact of rotational speed and axial feed on product hardness

The findings reveal that an increase in rotational speed results in greater hardness, primarily due to the repeated passage of forming balls over the same surface area. In contrast, as the axial feed increases, hardness decreases because the distance between successive ball impacts grows, reducing the cumulative effect of repetitive deformation on the part's surface as shown in Graphs 17 a, b. These results are in good agreement with the findings of [25].



(a)



(b)

**Graph 17** Effect die rotational speed on product hardness at thickness 4, 5 (mm)

#### 16 Conclusions

In the present study, metal-forming processes using ballizing technique (balls spinning). The results were conceptually analyzed to lead to some significant conclusions. Also, some topics in this area of present study are recommended to be investigated in the future work. The following are some drawn conclusions out of the results discussion.

The following conclusions can be extract from the present study:

- The process is a novel, simple, and cost-effective technique with low tooling requirements, making it a practical alternative to conventional forming methods. it is true, energy, time, and material saving Thus, the cost of production and product is saved.

- Die rotational speed, interference between forming balls and the sample (cross in feed), and axial feed significantly influence the forming load, filling rate, hardness, and overall product quality. Moreover, the optimal values of these parameters were determined, achieving lower forming loads and enhanced product quality.
- The axial load is greater than both the tangential and radial loads, with the tangential load being the smallest. Additionally, the forming load components increase as the interference (cross in-feed) and axial feed increase.
- The optimum die speeds were found to range between 200-315 rpm across all values of cross in-feed and axial feed. Additionally, the optimal specimen thickness was determined to be 5 mm when the cross in-feed is 0.7 times the specimen thickness, and the ideal axial feed was found to be 0.13 mm/rev.

#### Author Contributions

*The authors of this study have made significant contributions throughout the research process. Firstly, Mohamed N. El-Sheikh played a crucial role in designing the main idea of the study. Additionally, Emad A. Fahmy, Ahmed M.I. Abu-Oqail, Hammad T. Elmetwally, Eman S. M. Abd-Elhali and Ayman Ali Abd-Eltwab worked together to prepare the test-rig component, performed, and wrote a draft copy, collected the data and analyzed it. Ayman Ali Abd-Eltwab and Mohamed N. El-Sheikh review and revised the manuscript.*

#### Funding

*This research received no external funding.*

#### Conflicts of Interest

*The authors declare no conflict of interest.*

#### Acknowledgement

*The authors would like to extend acknowledgement to their research institutions Faculty of Engineering, Faculty of Technology and Education Beni-Suef University and Mechanical Eng. Dep., Faculty of Engineering, Assiut University, Assiut, Egypt, that provided support for this work.*

#### References

- [1] ZHANG, S. H., LI, M. S., XU, Y., KANG, D. C., & LI, C. Z. (2005). Introduction to a new CNC ball-spinning machine. *Journal of materials processing technology*, 170(1-2), 112-114.
- [2] MUSIC, O., ALLWOOD, J. M., & KAWAI, K. (2010). A review of the mechanics of metal spinning. *Journal of materials processing technology*, 210(1), 3-23.
- [3] KUSS, M., & BUCHMAYR, B. (2016). Damage minimised ball spinning process design. *Journal of materials processing technology*, 234, 10-17.
- [4] DYL, T. (2017). The numerical and experimental analysis of ballizing process of steel tubes. *Archives of Metallurgy and Materials*, 62(2A), 807-814.
- [5] DYL, T. (2017). The Numerical Analysis of the Ballizing Process. *Scientific Journal of Gdynia Maritime University*, (100), 63-75.
- [6] FATTOUH, M. (1989). Some investigations on the ballizing process. *Wear*, 134(2), 209-219.
- [7] EL-ABDEN, S. Z., ABDEL-RAHMAN, M., & MOHAMED, F. A. (2002). Finishing of non-ferrous internal surfaces using ballizing technique. *Journal of materials processing technology*, 124(1-2), 144-152.
- [8] KIM, N., KIM, H., & JIN, K. (2013). Minimizing the axial force and the material build-up in the tube flow forming process. *International Journal of precision engineering and manufacturing*, 14, 259-266.
- [9] ZHANG, G. L., ZHANG, S. H., LI, B., & ZHANG, H. Q. (2007). Analysis on folding defects of inner grooved copper tubes during ball spin forming. *Journal of materials processing technology*, 184(1-3), 393-400.
- [10] KHODADADI, M., KHALILI, K., & ASHRAFI, A. (2020). Studying the effective parameters on teeth height in internal gear flowforming process. *International Journal of Engineering*, 33(12), 2563-2571.
- [11] ABD-ELTWAB, A. A., EL-ABDEN, S. Z., AHMED, K. I., EL-SHEIKH, M. N., & ABDEL-MAGIED, R. K. (2017). An investigation into forming internally-spline sleeves by ball spinning. *International Journal of Mechanical Sciences*, 134, 399-410.
- [12] AYMAN A. ABD-ELTWAB, AHMED M. ALI KHAIR-ALLAH, A. M. ATIA, AND ESSAM K. SAIED, "A Novel Tool for Producing Externally Splined Sleeves." *International Journal of Scientific & Technology Research*, ISSN 2277-8616 Volume 9, Issue 06, June 2020.

- [13] RAGAB K. ABDEL-MAGIED, EMAD A. FAHMY, A. EL-SAYED M. HASSAN, MOHAMED N. EL-SHEIKH, ESSAM K. SAIED AND AYMAN A. ABD-ELTWAB, "An Investigation into Forming Externally Toothed Parts using Novel Tool based on Rotary Forging Technique." *International Journal of Advanced Science and Technology*, ISSN: 2005-4238 IJAST, Vol. 29, No.03, (2020), pp. 2194-2206.
- [14] ABD-ELTWAB, A.A., HELAL, G.I., EL-SHEIKH, M.N., SAIED, E.K., & ATIA, A.M. (2023). An Investigation into Conventional Spinning Process Using Ball Shaped Rollers as Forming Tool. *Manufacturing Technology Journal*, 23(6), 788-800. doi: 10.21062/mft.2023.084.
- [15] AYMAN ALI ABD-ELTWAB, GAMAL I. HELAL, AHMED ELSHEIKH, KARIM MOHAMED ATIA AND GOMAA A. A. (2023). The Influence of Roller Geometrical Shaped in Conventional Spinning Process. *Rare Metal Materials and Engineering*, ISSN 1002-185X & eISSN: 1875-5372, Vol. 52 Iss. 11.
- [16] ABD-ELTWAB, A.A., ELSYED AYOUB, W., EL-SHEIKH, M.N., SAIED, E.K., GHAZALY, N.M., & GOMAA, A.A. (2024). An Investigation into Forming of Gears Using Rotary Forging Process. *Manufacturing Technology Journal*, 24(4), 539-551. doi:10.21062/mft.2024.068.
- [17] ABD-ELTWAB, A.A., HAMDY, K., ELSHEIKH, A., SAIED, E.K., GHAZALY, N.M., & GOMAA, A.A. (2024). An investigation into production of double wall tube using squeeze Ballizing technique. *Journal of Manufacturing Processes*, 127 (2024) 545-558. <https://doi.org/10.1016/j.jmapro.2024.08.005>
- [18] AYMAN ALI ABD-ELTWAB, ESSAM KHALAF SAIED, AHMED MOHAMED ATIA, NOUBY M. GHAZALY, A.A. GOMAA, KARIM MOHAMED ATIA (2024). Investigation of externally toothed parts forming using ballizing technique. *Results in Materials*, 24 (2024) 100640. <https://doi.org/10.1016/j.rinma.2024.100640>.
- [19] BHATT, R. J., & RAVAL, H. K. (2018). In situ investigations on forces and power consumption during flow forming process. *Journal of Mechanical Science and Technology*, 32, 1307-1315.
- [20] AHMED, K. I. (2011). A new ball set for tube spinning of thin-walled tubular parts with longitudinal inner ribs. *JES. Journal of Engineering Sciences*, 39(1), 15-32.
- [21] CHUNJIANG, Z., GUANGHUI, L., JIE, X., ZHENGYI, J., QINGXUE, H., JIANMEI, W., & HAILONG, C. (2018). A quasi-dynamic model for high-speed ball spinning. *The International Journal of Advanced Manufacturing Technology*, 97, 2447-2460.
- [22] OH, J. T., LAI, M. O., & NEE, A. Y. C. (1993). Stress analysis of a ballised hole. *Journal of Materials Processing Technology*, 37(1-4), 137-147.
- [23] WANG, K. H., BLUNT, L. A., & STOUT, K. J. (1998). The 3-D characterisation of the surface topography of the ballizing process. *International Journal of Machine Tools and Manufacture*, 38(5-6), 437-444.
- [24] HAMMAD ELMETWALLY; EMAD FAHMY; EMAN S. M. ABD-ELHALIM; AHMED M.I. ABU-OQAIL; MOHAMED EL-SHEIKH; AYMAN ABD-ELTWAB. Production of externally gear parts with a new multi-level forming tool based on rotary ballizing technology using Numerical and experimental study. *Journal of Engineering Sciences*, 53, 3, 2025, 78-99. doi: 10.21608/jesaun.2025.356763.1416.
- [25] M. H. KASSAR, S. Z. EL-ABDEN, AND EL-SHEIKH, M. N. (November 2021). An Investigation of Tube Spinning Using Ballizing Technique, *International Journal of Scientific & Technology Research*, vol 10, ISSUE 11.
- [26] KHODADADI, MAJID. (29 Sep. 2025 ).Investigation of manufacturing bilayer gears using flow forming process to enhance the strength of gears. *Scientific reports* vol. 15,1 33627, doi:10.1038/s41598-025-19276-0.